Adsorption (2018) 24:769–779
https://doi.org/10.1007/s10450-018-9983-9

On the computer simulations of carbon nanoparticles porosity: statistical mechanics model for CO_2 and N_2 adsorption isotherms

Manel Bergaoui[1,2] · Chadlia Aguir[3] · Mohamed Khalfaoui[1,2] · Jhonny Villarroel-Rocha[4] · Laurence Reinert[5] · Eduardo Enciso[6] · Laurent Duclaux[5] · Deicy Barrera[4] · Karim Sapag[4]

Received: 15 July 2018 / Revised: 1 October 2018 / Accepted: 9 October 2018 / Published online: 12 October 2018

Abstract
A new approach model was developed for the pore size characterization of carbon porous materials, using adsorption gases. The experimental adsorption isotherms of CO_2 and N_2 onto carbon nanoparticles were used to test the validity of such model. The Trimodal-Gauss-Monolayer model has been found to adjust well the experimental data of CO_2 sorption at 273 K and has allowed detect the ultra-micropores till 0.7 nm. For the mesopores and macropores, it has been concluded that the N_2 sorption isotherms at 77 K are suitable to characterize this kind of porosity. These isotherms have been well fitted with the Gauss-Monolayer/Gauss-Finite Multilayer model derived from the same approach. Thereby, the novel method can be used as a generalized technique for the simulation of type IVa isotherms. Indeed, this novel method agreed with other methods, NLDFT, QSDFT, and VBS available for pore size distribution.

Keywords Carbon nanoparticles · Pore size distribution · Statistical mechanics modeling · N_2 adsorption/desorption and CO_2 adsorption isotherms

1 Introduction

Carbon materials are widely used in many applications such as drug delivery and other medical uses due to their small diameters and ability to penetrate cells and tissues (Nagaraju et al. 2015; Zhang et al. 2009, 2017; Prehal et al. 2017; Przepiórski et al. 2013). The porous texture, i.e., pore volume and pore size distribution (PSD) is an important characteristic that controls their properties (Tao et al. 2009; Wongkoblap et al. 2010; Jahandar Lashaki et al. 2016). Therefore, the characterization of the porous texture is required to predict and understand the performance of an adsorbent, as studied by many researchers (Tao et al. 2009; Chu et al. 2014; Guillet-Nicolas et al. 2016; Reichhardt et al. 2012; Seo et al. 2015; Zhang et al. 2013).

The analysis of nitrogen adsorption/desorption measured at 77 K is known to be an efficient tool to evaluate the PSD using several methods/models (Gregg and Sing 1982; Rouquerol et al. 1999). However, the diffusion of N_2 molecules at 77 K into carbon micropores is very slow (Jagiello and Thommes 2004). Furthermore, at this temperature, it was emphasized out that the diffusional limitations might influence the adsorption in ultra-micropores, i.e., pores smaller than 0.7 nm (Rodriguez-Reinoso and Linares-Solano 1988). This leads to time-consuming measurements and can cause under-equilibration of measured adsorption isotherms, especially, for porous carbons which contains a large range of pore sizes including ultra-micropores (Jagiello and Thommes 2004). Nevertheless, these problems have been

✉ Mohamed Khalfaoui
mohamed.khalfaoui@isimm.rnu.tn

1 Department of Technology, Materials Sciences, Microelectronics and Nanotechnologies Research Group, Higher Institute of Computer Sciences and Mathematics of Monastir, University of Monastir, 5000 Monastir, Tunisia

2 Physico-Chemical Materials Laboratory LR01ES19, Department of Physics, Faculty of Sciences of Monastir, University of Monastir, 5000 Monastir, Tunisia

3 Research Unit of Applied Chemistry and Environment UR13ES63, Faculty of Sciences of Monastir, University of Monastir, 5000 Monastir, Tunisia

4 Laboratorio de Solidos Porosos, Instituto de Física Aplicada, Universidad Nacional de San Luis, CONICET, Ejercito de los Andes 950 2do Piso, Bloque II, 5700 San Luis, Argentina

5 Laboratory of Molecular Chemistry and Environment, University Savoie Mont Blanc, 73000 Chambery, France

6 Department of Physical Chemistry I, Faculty of Chemical Sciences, Complutense University, 28040 Madrid, Spain

overcome by using carbon dioxide adsorption analysis at 273 K (Garrido et al. 1987) as it was proposed by Rodriguez-Reinoso et al. (1988). Indeed, at 273 K of temperature, CO_2 molecules can access more easily the ultra-micropores than N_2 at 77 K despite that the critical molecular dimensions of both gases (N_2—3.64 Å, CO_2—3.30 Å) are similar (Jagiello and Thommes 2004; Joshi et al. 2007).

The widely used methods for the characterization of pore structure of carbons and other porous materials are the microscopic methods such as Monte Carlo (MC) (Wongkoblap et al. 2010), molecular dynamics (MD) (Gelb and Gubbins 1999) simulations, non-local density functional theory (NLDFT) (Landers et al. 2013; Li et al. 2014), quenched solid density functional theory (QSDFT) (Neimark et al. 2009), and two-dimensional density functional theory (2D-DFT) models (Jagiello and Olivier 2013); and the macroscopic methods such as the ones of Barrett, Joyner and Halenda (BJH) (Barrett et al. 1951), Pierce (1953), Dollimore and Heal (DH) (Dollimore and Heal 1970), Kruk, Jaroniec and Sayari (BJH–KJS) (Kruk et al. 1997). A macroscopic method referred to Villarroel–Barrera–Sapag (VBS) was also proposed to evaluate the PSD of mesoporous materials taking into account the correct filling/emptying mechanism of each type of pores as an improvement of the BJH and DH methods (Villarroel-Rocha et al. 2011, 2014). All the above mentioned methods could be used considering the specific physics considerations of each one and its restrictions. Nevertheless, as it is known, DFT method provides reliable information about the pore size distribution of different materials in the entire range of pore sizes (Nakhli et al. 2014).

In our previous work (Bergaoui et al. 2016), a new integral equation named Gauss-Monolayer/Gauss-Modified BET (GM/GMBET) model was developed for PSD prediction from N_2 adsorption/desorption isotherms of type II or III according to IUPAC classification (Nakhli et al. 2014) and applied to the case of polystyrene and its copolymers. The local isotherms used in this previous work are the monolayer and the modified BET models (Khalfaoui et al. 2003) in which monolayer filling mechanism and infinite capillary condensation are taken into consideration. These two models based on statistical physics simulation (SPS) method involve parameters having physical significance, unlike empirical models.

In this work, the GM–GMBET method was extended to the simulation of type IVa isotherms, like the ones of carbon nanoparticles (CNPs). This isotherm type, at low relative pressures is similar to type II. Therefore, the monolayer model was used as a local isotherm. However, at high relative pressures, the application of the modified BET model (Bergaoui et al. 2016; Khalfaoui et al. 2003) has limitations for this type IVa isotherm which does not possess any saturation level (the plateau in the isotherm). Thus, the finite multilayer model (Nakhli et al. 2014) was used as a local isotherm considering a capillary condensation that is having a saturation level unlike an infinite capillary condensation from the classical BET model.

As it was mentioned, the CO_2 adsorption isotherms at 273 K (type Langmuir) allow to achieve a complete characterization of CNPs beside the N_2 data at 77 K, and considering that some studies, using molecular simulation (Seaton and Walton 1989; Tan and Gubbins 1990, 36) and experimental data (Kaneko et al. 1989; Kakei et al. 1990) has suggested a monolayer formation even in micropore filling, in this work the PSD from CO_2 isotherms data was also obtained by using the same statistical physics approach.

2 Methods

2.1 Experimental measurements

Three CNPs samples representing different pore structures denoted C_1NPs, C_2NPs, and C_3NPs were analyzed using adsorption isotherms of N_2 at 77 K and CO_2 at 273 K. These studied carbon nanoparticles have been prepared from organic resins in aqueous solution following the approach of Pekala (1989) and according to the procedures developed by Barroso-Bujans et al. (2014). The carbon nanoparticles were obtained by the pyrolysis of the organic resin at 900 °C for 4 h in a nitrogen atmosphere using a heating rate of 3 °C/min and a cooling rate of 5 °C/min. Indeed, to obtain nanoparticles with different pore structure, the reactions were performed at different pH by adding appropriate amounts of sodium hydroxide and keeping the Resorcinol (R)-to-Formaldehyde (F) molar ratio (R/F) at 0.5 (Barroso-Bujans et al. 2014). Adsorption isotherms of N_2 and CO_2 were measured using manometric adsorption equipment (ASAP 2020, Micromeritics). Before the adsorption measurements, the samples were outgassed for 6 h at 250 °C. From N_2 adsorption data, the specific surface area (S_{BET}) and the total pore volume (V_T) were calculated by the Brunauer–Emmet–Teller (BET) method following the IUPAC recommendations (Thommes et al. 2015) and Gurvich's rule (Rouquerol et al. 2013), respectively, for all samples. The α_s-plot method (Gregg and Sing 1982) was used to calculate the micropore volume ($V_{\mu p}$) and the external surface area (S_{ext}) using the GCB-1 non porous carbon as a reference adsorbent (Nakai et al. 2010). The mesopores volume (V_{meso}) was obtained from the difference between V_T and ($V_{\mu p}$).

The PSD was obtained using the macroscopic VBS method (Villarroel-Rocha et al. 2011, 2014). This method is an improved BJH one (Barrett et al. 1951) using a f_c correction term obtained by fitting the experimental isotherm with a set of simulated isotherms. In the present study, the VBS

method was applied in the relative pressure range from 0.05 to 0.98. The PSDs from the QSDFT and the NLDFT were also compared with those derived from the VBS method. These last methods are included in ASiQwin software, v. 4.0 (Quantachrome instruments).The kernel selected for QSDFT method was N_2 at 77 K on carbon slit/cylindrical pores (Neimark et al. 2009). For NLDFT method, the selected kernel was CO_2 at 273 K on carbon slit pores (Ravikovitch et al. 2000).

2.2 Assumptions model

The new theoretical model has been developed based on the following assumptions:

I. The adsorption process involves a successive monolayer formation followed by a multilayer formation.
II. The same adsorption process is assumed in all the pores range, based on previous experimental and simulation studies mentioned above.
III. Any pore geometry is considered due to the proposed model is based on classical thermodynamics.
IV. In the case of PSD evaluation from CO_2 adsorption data the proposed model assumes a heterogeneous microporosity considering three kinds of micropores (ultramicropores, and narrow and larger supermicropores). Therefore, a trimodal Gaussian distribution function is used.

2.3 Theoretical approach and simulation method

By using the newest methods, the PSD is calculated from an equation in which the experimental isotherm is the integral of the local pore isotherm multiplied by the pore size distribution as (Seaton and Walton 1989):

$$Q_a(p) = \int_{\omega_{min}}^{\omega_{max}} f(\omega).Q_{a-LI}(p,\omega)d\omega \quad (1)$$

where $Q_a(p)$ is the adsorbed quantity at a pressure p, ω_{min} and ω_{max} are the minimum and the maximum pore size, respectively, and $Q_{a-LI}(p,\omega)$ is the adsorbed quantity of the local/kernel isotherm at pressure p and a pore size ω. The pore size distribution, $f(\omega)$, is the distribution of the pore volume as a function of the pore size.

For nitrogen adsorption isotherms on materials with large mesopores or narrow macropores, the monolayer is usually completed at relative pressures lower than 0.35, and at higher values, the number of adsorbed layers could go to infinity. These materials present type II isotherms, where the adsorbed amount quickly increases at high relative pressures close to 1. To evaluate the PSD of this type of materials (Bergaoui et al. 2016), we have proposed a method named GM/GMBET based on the description of the whole isotherm by two local isotherm branches using a monolayer and a modified BET models (Khalfaoui et al. 2003). In this previous work, the filling mechanism of the monolayer and the infinite capillary condensation were taken into consideration.

For the type IVa isotherms, the similarity at low relative pressure branch with type II isotherm leads us to use a monolayer model as a local one. Moreover, the characteristic features of the type IVa isotherm are on the one hand its hysteresis loop, owing to the capillary condensation of the adsorbate in the mesopores, and on the other hand, the saturation uptake achieved (the plateau) at high relative pressure (Sing 1985). Therefore, the modified BET model (Bergaoui et al. 2016; Khalfaoui et al. 2003) cannot be applied for this kind of isotherms (type IVa), because it does not specify a saturation level. Thus, at high relative pressure, an analytical expression was used describing the physisorption when the number of adsorbed layers is greater than unity and finite. This finite multilayer model is addressing the above limitation and can be used as a local isotherm with a saturation level (Nakhli et al. 2014), introducing the number of adsorbed layers as a fitting parameter.

Firstly, a statistical physics simulation (SPS) was realized to determine the local isotherm parameters, and secondly, an integral equation procedure was applied to evaluate the PSD.

2.3.1 Local isotherms

Each set of equilibrium data was correlated with pure-species equilibrium numerical models. Two different expressions of the local isotherms have been used for N_2 and CO_2 adsorption: the monolayer (M) (Khalfaoui et al. 2003) and the finite multilayer (FM) (Nakhli et al. 2014) models.

For the monolayer adsorption model, the receptor site can be empty ($N_i = 0$) or occupied once ($N_i = 1$). Then, the partition function of one receptor site is written as (Khalfaoui et al. 2003):

$$z_{gc} = 1 + e^{-\beta(\varepsilon-\mu)} \quad (2)$$

where ε (kJ) is the adsorption energy of the receptor site, μ (kJ) is the chemical potential, and β is defined as being $(1/k_BT)$, where k_B is the Boltzmann's constant.

The dependence between the adsorption energy, ε, and the pore size can be expressed as (Bergaoui et al. 2016; Rouquerol et al. 2013; Sun 2002):

$$\varepsilon = \frac{\mathcal{K}}{w} \quad (3)$$

where $\mathcal{K}$ (kJ nm/mol) is a characteristic constant for a defined adsorbate/adsorbent system and w (nm) is the pore size.

This leads to the following expression of the adsorbed amount, Q_{a-M}:

$$Q_{a-M}Q_{a-m}\left(\frac{p}{p^0},w\right)=\frac{n\times N_m}{1+e^{\frac{\mathcal{K}}{wRT}}\left(\frac{p^0}{p}\right)^n} \tag{4}$$

where n is the number of the adsorbed molecule(s) per site, N_m ($\mathrm{cm^3\,liq\,g^{-1}}$) is the receptor sites density, R (8.314 J/K mol) is the universal gas constant, T (K) is the absolute temperature and $\frac{p}{p^0}$ is the relative pressure.

If the adsorption occurs with a capillary condensation followed by a saturation level, the receptor site can be empty ($N_i=0$), occupied once ($N_i=1$), twice ($N_i=2$), etc., up to $N_i=N_\ell$, where N_ℓ is the average number of the adsorbed layers. In such case, the grand canonical partition function is written as:

$$z_{gc}=\sum_{N_i=0}^{N_\ell}e^{-\beta N_i(\varepsilon_i-\mu)}=1+e^{-\beta(\varepsilon_1-\mu)}\times\left[\frac{1-e^{-N_\ell\beta(\varepsilon_2-\mu)}}{1-e^{-\beta(\varepsilon_2-\mu)}}\right] \tag{5}$$

where $\varepsilon_{i=1,\,2}$ (kJ) is the adsorption energy for the first layer ($i=1$) and the second one ($i=2$).

Accordingly, the amount adsorbed, Q_{a-FM}, is given by the following expression:

$$Q_{a-FM}\left(\frac{p}{p^0},\,w\right)=n\times N_m\times\frac{e^{-\mathcal{K}/wRT}\left(\alpha.\frac{p}{p^0}\right)^n\left(1-\left(N_\ell+1\right)\left(\frac{p}{p^0}\right)^{nN_\ell}+N_\ell\left(\frac{p}{p^0}\right)^{n(N_\ell+1)}\right)}{\left[1-\left(\frac{p}{p^0}\right)^n+e^{-\mathcal{K}/wRT}\left(\alpha.\frac{p}{p^0}\right)^n\times\left(1-\left(\frac{p}{p^0}\right)^{nN_\ell}\right)\right]\left[1-\left(\frac{p}{p^0}\right)^n\right]} \tag{6}$$

with α as constant, $\left(\alpha=e^{\varepsilon_L/RT}\right)$ such as ε_L (valid for the second and higher layers) is equal to the liquefaction heat as assumed by the finite multilayer (FM) model (Nakhli et al. 2014). Indeed, it is assumed that each layer is anchored with an adsorption energy level $\varepsilon_{N_\ell}=\left[\varepsilon+\left(N_\ell-1\right).\varepsilon_L\right]$, where ε is the monolayer adsorption energy due to the adsorbent-adsorbate interaction and ε_L is an adsorption energy related to the adsorbate–adsorbate interaction (Nakhli et al. 2014).

2.3.2 Integral procedure: PSD evaluation

Equations (4) and (6) have been extended for predicting the pore size distribution from N_2 and CO_2 adsorption equilibrium data, by assuming a PSD function $f(w)$. The adsorption energy distribution function most commonly used is Gaussian (Leo 1994). Thus the pore size distribution, $f(w)$, is written as follows:

$$f(w)=f_0\times\frac{\mathcal{K}}{w^2\sigma\sqrt{2\pi}}\exp\left(-\frac{\left(1/w-1/w^0\right)^2\times\mathcal{K}^2}{2\sigma^2}\right) \tag{7}$$

where f_0 is the fraction of the pore volume, w^0 is the average pore size and σ is the dispersion of the Gaussian distribution.

For N_2 adsorption/desorption isotherms, the integral equations using the monolayer model in the first region of relative pressure (i.e., up to 0.35) and the finite multilayer model in the second region (between 0.35 and 0.99) as local isotherms to fit our experimental data, can be written as follows in Eqs. (8) and (9), respectively:

$$Q_{a-GM}\left(\frac{p}{p^0}\right)=\int_{\omega_{min}}^{\omega_{max}}f_1(\omega)\cdot Q_{a-M}\left(\frac{p}{p^0},\omega\right)d\omega \tag{8}$$

$$Q_{a-GFM}\left(\frac{p}{p^0}\right)=\int_{\omega_{min}}^{\omega_{max}}f_2(\omega)\cdot Q_{a-FM}\left(\frac{p}{p^0},\omega\right)d\omega \tag{9}$$

where $f_1(\omega)$ and $f_2(\omega)$ have the same expression of $f(w)$ with different fractions of pore volume, f_1 and f_2 (instead of f_0), are related to the first and second peaks, respectively. $w_{\min}$ and $w_{\max}$ are the minimum and the maximum pore size, respectively.

Then, the N_2 adsorption equilibrium data in each segment were fitted dependently with the sum of GM (Eq. 8) and GFM (Eq. 9) models:

$$Q_a\left(\frac{p}{p^0}\right)=Q_{a-GM}\left(\frac{p}{p^0}\right)+Q_{a-GFM}\left(\frac{p}{p^0}\right) \tag{10}$$

Equation (10) resumes the use of the Gauss-Monolayer/Gauss-Finite Multilayer (GM/GFM) model.

For CO_2 adsorption isotherms, the prediction of PSD was evaluated by using the Eq. (4) as local isotherm. This equation was coupled with a trimodal Gaussian distribution function allowing us to use the following equation:

$$Q_a\left(\frac{p}{p^0}\right)=Q^1_{a-GM}\left(\frac{p}{p^0}\right)+Q^2_{a-GM}\left(\frac{p}{p^0}\right)+Q^3_{a-GM}\left(\frac{p}{p^0}\right) \tag{11}$$

where $Q^{i=1,2,3}_{a-GM}\left(\frac{p}{p^0}\right)=\int_{\omega_{imin}}^{\omega_{imax}}f_i(\omega_i).Q_{a-M}\left(\frac{p}{p^0},\omega_i\right)d\omega_i$

It can be noted that the trimodal PSD corresponds to three pore volume fractions: f_1, f_2 and f_3. Equation (11) resumes the application of the Trimodal-Gauss-Monolayer (Trimodal-GM) model.

Finally, the N_2 adsorption equilibrium data were fitted with GM/GFM model, and the CO_2 adsorption isotherms were fitted with Trimodal-GM model, by minimizing the sum of the squares of the errors (ERRSQ) (Chan et al. 2012):

$$ERRSQ = \sum_{i=1}^{j} \left(Q_{calc} - Q_{meas}\right)_i^2 \quad (12)$$

where Q_{calc} is the theoretical adsorbed amount calculated according tothe local isotherm models, Q_{meas} is the experimentally determined adsorbed amount and j is the number of data points.

The corresponding absolute relative error (ARE) values were estimated from Eq. (13) (Kapoor and Yang 1989), and the optimum fitting parameters were obtained.

$$ARE\ (\%) = \frac{100}{j} \sum_{i=1}^{j} \left| \frac{Q_{calc} - Q_{meas}}{Q_{meas}} \right|_i \quad (13)$$

Then, the PSD has been obtained by a fitting procedure based on the solver add-in of Microsoft Excel (Microsoft Corporation 2007), which is based on the Generalized Reduced Gradient algorithm with nonlinear optimization.

3 Results and discussion

3.1 Experimental isotherms and textural properties

Nitrogen adsorption/desorption isotherms at 77 K for C_1NPs, C_2NPs, and C_3NPs samples are depicted in Fig. 1. According to the IUPAC classification, all materials exhibited type IVa isotherms and present hysteresis loops which are typical of mesoporous materials (Sing 1985; Barrera et al. 2011). The isotherms of C_2NPs and C_3NPs samples exhibit an H1 type hysteresis loop while in the isotherm of C_1NPs the H2 type hysteresis loop closes at 0.4 p/p^0 indicating the presence of cavitation phenomena on the desorption branch (Villarroel-Rocha et al. 2014).

The CO_2 adsorption capacity of the porous carbon nanoparticles was measured at 273 K, as shown in Fig. 2. All the isotherms are Langmuir type, and typical of adsorbents having micropores.

Table 1 shows the measured density (ρ) of each sample and the textural properties determined from N_2 adsorption–desorption isotherms data at 77 K of carbon nanoparticles. The density was calculated from the following

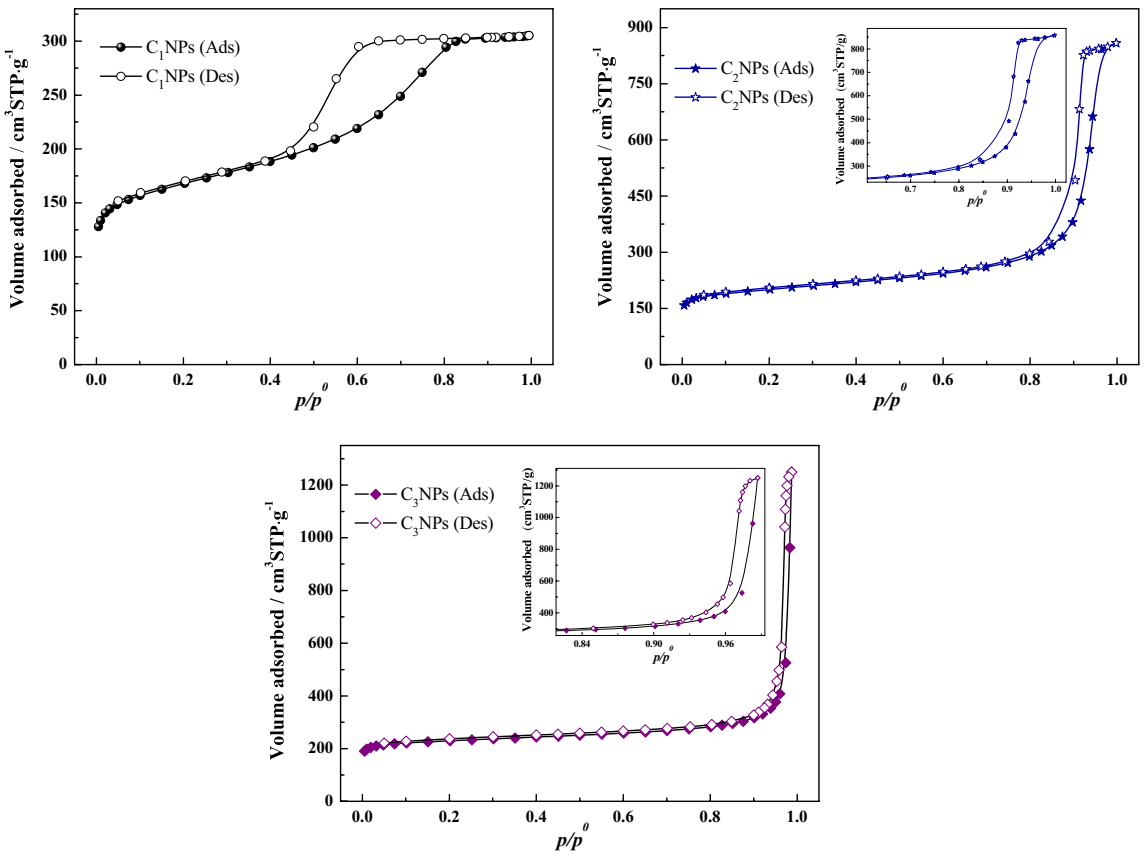

Fig. 1 The N_2 adsorption–desorption isotherms at 77 K of all the carbon nanoparticles samples (filled symbol: adsorption; empty symbol: desorption)

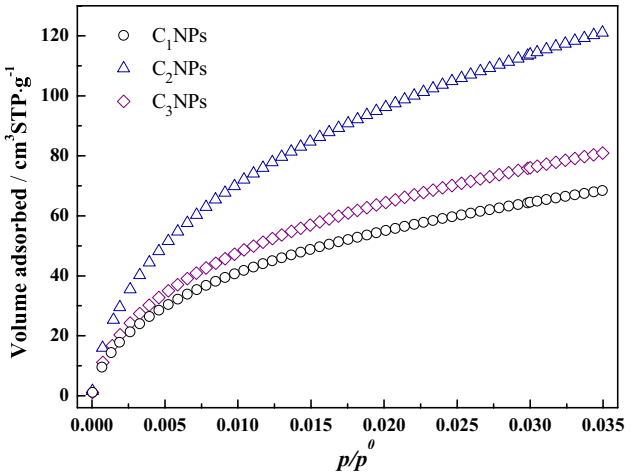

Fig. 2 CO_2 adsorption isotherms at 273 K of the carbon nanoparticles samples

Table 1 Textural properties of the CNPs samples obtained from N_2 adsorption/desorption isotherms

Material	C_1NPs	C_2NPs	C_3NPs
ρ (g/cm^3)	0.75	0.50	0.38
S_{BET} (m^2/g)	610	755	620
V_T (cm^3/g)	0.47	1.33	1.93
V_{meso} (cm^3/g)	0.35	1.17	1.80
$V_{\mu p}$ (cm^3/g)	0.12	0.16	0.13
S_{ext} (m^2/g)	175	170	170

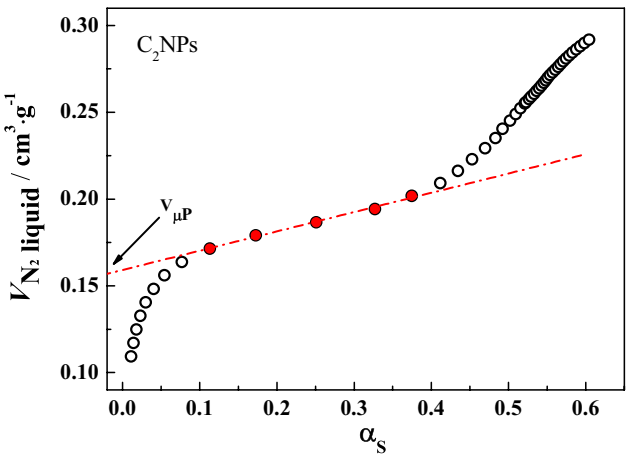

Fig. 3 α_s-plot curve (from N_2 adsorption data) of the C_2NPs sample. Filled symbols represent the selected range of α_s values

equation (Zeller et al. 2012): $\rho = \frac{1}{\left(V_T + \frac{1}{\rho_c}\right)}$, where V_T is the total adsorbed nitrogen according Gurvich's rule and ρ_c is

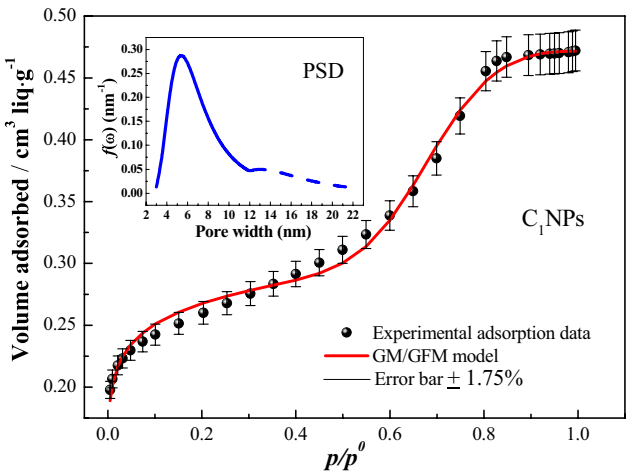

Fig. 4 N_2 experimental and theoretical isotherms and PSD of C_1NPs sample. The symbols are the experimental data; the solid lines are the fitted isotherms with GM/GFM model. Error bars represent 96.5% confidence intervals

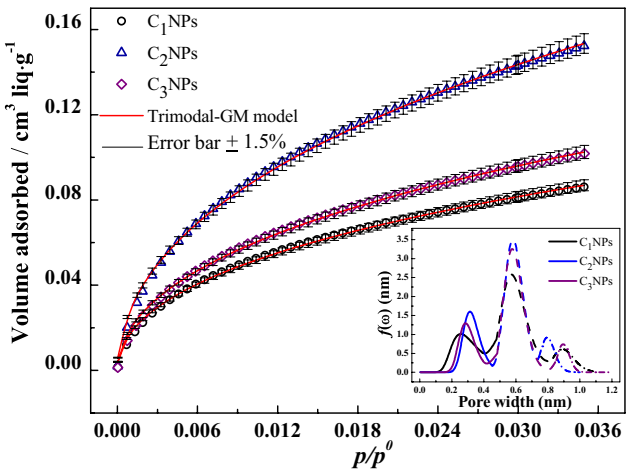

Fig. 5 CO_2 experimental and theoretical isotherms and PSD of all the samples. The symbols are the experimental data; the solid lines are the fitted isotherms with Trimodal-GM model. Error bars represent 97% confidence intervals

the density of non-porous carbon (1.9 g/cm^3) (Grehov et al. 2017). Figure 3 shows the α_s-plot curve (from N_2 adsorption data) for the C_2NPs sample exhibiting the presence of micropores, and same profiles have been obtained for the other samples. From the slope of the linear region of the α_s -plot curve, the external surface area (S_{ext}) of these three samples have been determined. After the linear region, a quick increase in the adsorbed volume is observed at higher α_s values (Fig. 3) due to the capillary condensation of N_2 in the mesopores (Huang et al. 2014). Furthermore, the total pore volume increases as decreasing the density of samples showing that C_3NPs is the most porous sample with the

Table 2 Fitting parameters obtained by using the proposed models for all samples

	p/p^0 segment	Parameter	C_1NPs	C_2NPs	C_3NPs
			Adsorption branch	Desorption branch	
N_2	GM model	n	0.102	0.147	0.151
		N_m (cm^3 liq/g)	5.024	5.05	6.027
		w_{min} (nm)	3	2	2
		w_{max} (nm)	12	36	65
		σ (kJ/mol)	0.709	0.582	0.141
		$\mathcal{K}$ (kJ nm/mol)	11.233	25	15
		w^0 (nm)	6.927	23.927	31.053
		f_1	1.656	0.968	0.276
	GFM model	n	9.349	150.217	180
		N_m (cm^3 liq/g)	0.069	0.036	0.011
		N_ℓ	0.544	1.034	0.626
		w_{min} (nm)	11.283	35	50
		w_{max} (nm)	21.977	55	125
		σ (kJ/mol)	0.34	0.077	0.01
		α	1.721	1.106	1.035
		$\mathcal{K}$ (kJ nm/mol)	17	12.084	5
		w^0 (nm)	15.024	41.975	75
		f_2	0.484	0.284	0.801
	GM model (Q^1_{a-GM})	ARE (%)	1.638	4.709	7.932
		n_1	0.485	1.465	0.498
		N_{1m} (cm^3 liq/g)	0.695	0.506	1.2
		w_{1min} (nm)	0.003	0.003	0.005
		w_{1max} (nm)	0.658	0.659	0.665
		σ_1 (kJ/mol)	5.05E−05	2.92E−05	3.38E−05
		$\mathcal{K}_1$ (kJ nm/mol)	3.70E−05	6.05E−05	5.86E−05
		w_1^0 (nm)	0.329	0.324	0.298
		f_1	0.285	0.213	0.172
CO_2	GM model (Q^2_{a-GM})	n_2	2.258	3	3
		N_{2m} (cm^3 liq/g)	0.29	0.5	0.814
		w_{2min} (nm)	0.3	0.3	0.2
		w_{2max} (nm)	0.987	0.987	0.987
		σ_2 (kJ/mol)	0.235	0.235	0.235
		$\mathcal{K}_2$ (kJ.nm/mol)	1.048	1.5	1.4
		w_2^0 (nm)	0.589	0.589	0.586
		f_2	0.507	0.507	0.503
	GM model ((Q^3_{a-GM}))	n_3	0.5	0.1	2.123
		N_{3m} (cm^3 liq/g)	0.2	0.2	0.352
		w_{3min} (nm)	0.8	0.7	0.6
		w_{3max} (nm)	1.1	1	1.2
		σ_3 (kJ/mol)	0.8	1	0.1
		$\mathcal{K}_3$ (kJ nm/mol)	10	15	2.5
		w_3^0(nm)	0.9	0.8	0.898
		f_3	0.1	0.1	0.069
		ARE (%)	4.564	5.169	5.165

highest mesopore volume (Table 1). Moreover, this sample presents a lower specific surface area compared to C_2NPs despite its important total pore volume.

3.2 Estimation of PSD from a simulation of N_2 and CO_2 adsorption isotherms

Pore size distribution of porous materials whose isotherms present hysteresis loop H1 type must be evaluated with desorption branch data due to it reflects transitions near the equilibrium phase (Villarroel-Rocha et al. 2011, 2014; Barrera et al. 2011). However, those ones that present hysteresis loop H2 type closing near 0.40–0.45 of relative pressure must be evaluated with adsorption branch data due to it presents the cavitation phenomenon. Thus, PSD evaluation of C_2NPS and C_3NPS, and C_1NPS were evaluated with the desorption and adsorption branches, respectively.

The PSDs of the three samples have been determined from N_2 and CO_2 isotherms using the GM/GFM and the Trimodal-GM models, respectively. Figure 4 reports the experimental N_2 adsorption isotherm for C_1NPs, along with the fitted isotherm using the GM/GFM model. This model assumes the monolayer formation in the first region (i.e., up to 0.35) and the subsequent finite multilayer phenomenon occurring between 0.35 and 0.99 of relative pressure, as previously described (theoretical section). Good fit to the C_1NPs experimental data (Fig. 4) is observed and the PSD was obtained from the fitting procedure. Figure 5 shows the fitted isotherms using Trimodal-GM model of the experimental CO_2 adsorption isotherms for all samples. Good fit to the experimental isotherm is also observed (Fig. 5), and the PSDs were calculated for all samples from the fitting procedure. Adjustment parameters obtained from the fitted N_2 and CO_2 isotherms of all the samples using GM/GFM and Trimodal-GM models are shown in Table 2.

According to Table 2, the values of ARE are small for all studied samples and do not exceed 8% for both GM/GFM and Trimodal-GM models. It can be noticed that the two fractions, f_1 and f_2, contribute to the Gauss-Monolayer and the Gauss-Finite Multilayer models, respectively. At low pore size range, the Gauss-Monolayer model is dominant (the value of f_1 is higher than f_2) except for C_3NPs. In that region, the average pore sizes, w^0, are equal to 6.9 nm, 23.9 nm and 31 nm for C_1NPs, C_2NPs and C_3NPs, respectively (Table 2). For the second pore sizes range, the Gauss-Finite Multilayer model is dominant for C_3NPs (the value of f_2 is higher than f_1) and the average pore size values are equal to 15, 42 and 75 nm for C_1NPs, C_2NPs and C_3NPs, respectively. These results confirms that the studied samples C_1NPs and C_2NPs are mainly mesoporous (the values of w^0 are smaller than 50 nm) and that the C_3NPs sample has got larger mesopores and/or narrow macropores (w^0 is about 75 nm). Moreover, for the first region (i.e., up to $p/p^0 = 0.35$), the n value lower than 1 confirms a monolayer where the adsorbed molecule is multi-anchored with different interactions sites. For the second region ($p/p^0 > 0.35$) simulation, the calculated n value higher than 1 reflects the multimolecular adsorption by the capillary condensation/evaporation of N_2. This occurs in mesopores for C_1NPs and C_2NPs, or on narrow macropores for C_3NPs. The

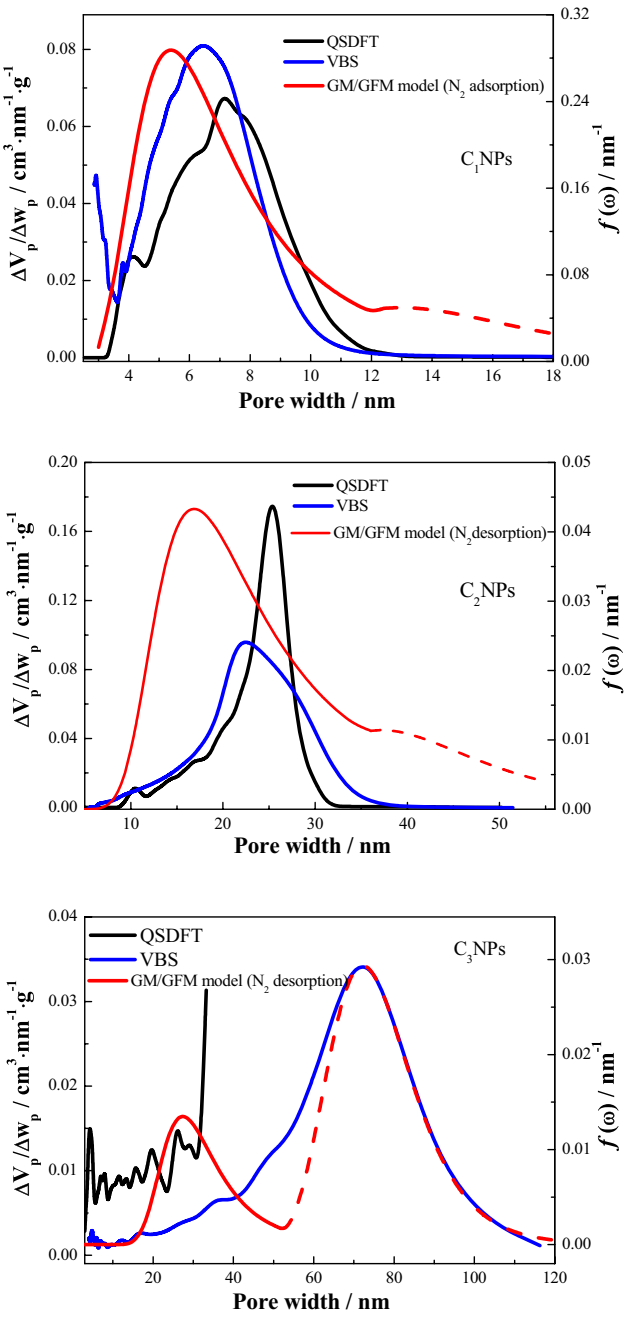

Fig. 6 Comparison of the PSDs of all the samples obtained by the VBS and the NLDFT methods and by the proposed GM/GFM model from adsorption (C_1NPs) and desorption branches (C_2NPs and C_3NPs)

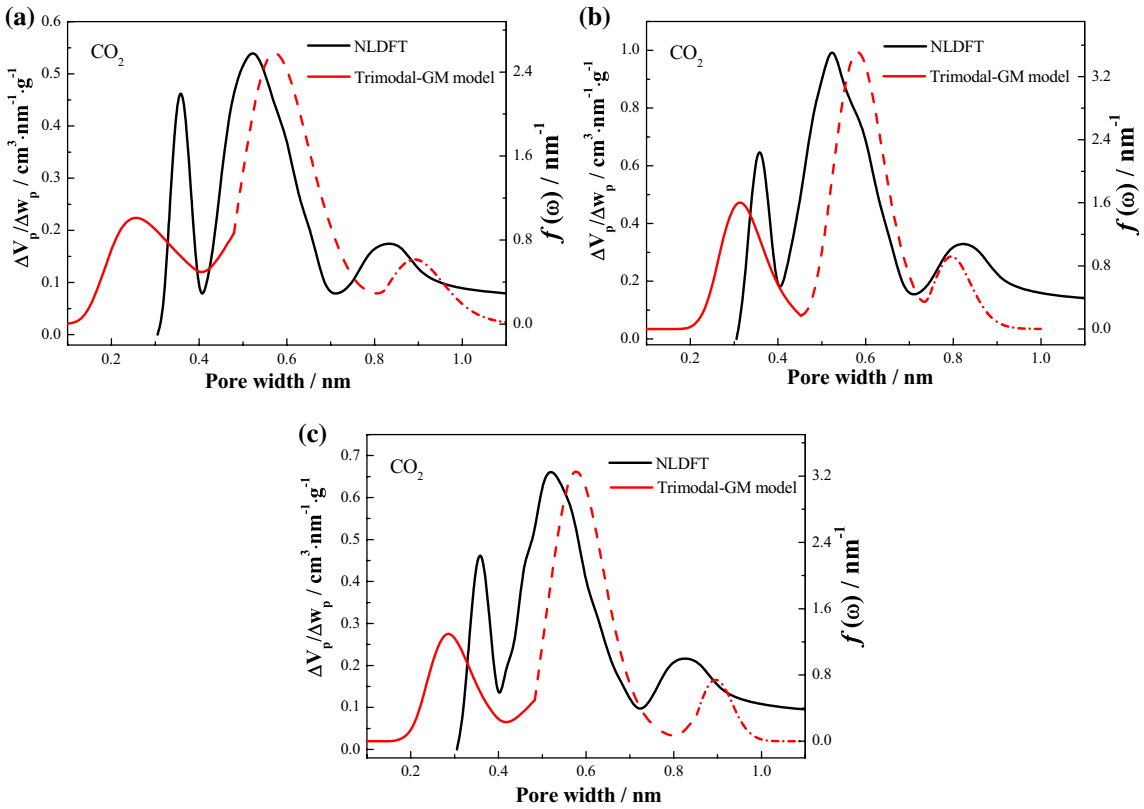

Fig. 7 Comparison of the PSDs of all the samples (**a** C_1NPs, **b** C_2NPs and **c** C_3NPs) obtained by the NLDFT method and by the proposed Trimodal-GM model

number of adsorbed layers, N_ℓ (characterizing the finite multilayer model ranging from 0.544 to 1.034) is given in Table 2. This parameter does not exceed the unity as it characterizes the number of adsorbed layers locally in each pore size.

According to the Trimodal-GM model, the average pore size, w^0, corresponds to an important fraction of pore volume in the second peak for all the samples (Table 2). This result indicates that the main peak of the average pore size is about 0.6 nm which corresponds to the micropore domain for all the studied samples. Furthermore, at this peak, the n fitted parameter higher than 1, cannot indicate a multimolecular adsorption as the monolayer is not achieved in this CO_2 pressure range. These high n values could be attributed to the CO_2 adsorption at 273 K (in micropores) via a volume-filling mechanism (Sevilla et al. 2013).

For all the samples, the PSDs obtained by the proposed GM/GFM model were compared with the QSDFT method and the VBS one (Fig. 6). Whatever the sample type, the PSDs from the GM/GFM model, the VBS and the QSDFT ones are almost similar. As it is known, DFT methods can be applied for evaluation the PSD over a wide range of pore sizes (ultramicropore to macropores). However, in our case the QSDFT method cannot detect any peak corresponding to the narrow macropores (~ 70 nm) as is shown in Fig. 6 for C_3NPs sample, where their isotherm presents the capillary evaporation step at $p/p^0 > 0.96$. So, the absence of this peak is due to the available kernel from the software (slit pore in the micropores region and cylindrical pore in the mesopores region) takes into account relative pressure values up to 0.93.

In the case of PSDs obtained from CO_2 adsorption, a good approach was found between the PSDs obtained by the Trimodal-GM model with those obtained by the NLDFT microscopic method (Fig. 7).

As a conclusion, the proposed models give suitable approximations of the PSD in materials having type I and IVa isotherms. The two proposed models have the advantage to describe PSDs in all the pore size domain explored by the QSDFT, the NLDFT and the VBS methods. Thus, this investigation leads us to highlight the importance of the Grand Canonical formalism in statistical mechanics description of gas adsorption.

4 Conclusion

The Trimodal-Gauss-Monolayer and the Gauss-Monolayer/Gauss-Finite Multilayer models have been developed by incorporating Gaussian pore size distribution and

local isotherms derived from statistical mechanics theory. These theoretical models have been used to evaluate the PSDs of carbon nanoparticles from N_2 adsorption/desorption and CO_2 adsorption isotherms. The adsorption data for both CO_2 at 273 K and N_2 at 77 K of carbon nanoparticles have been simultaneously well fitted by using the developed models that are in agreement with other methods (DFT and VBS) available for pore size distribution. The following key results are achieved:

I. N_2 adsorption/desorption and CO_2 adsorption experimental data were used to evaluate the PSD of three carbon nanoparticles samples, C_1NPs, C_2NPs, and C_3NPs in all the pore sizes range through the Trimodal-GM and GM/GFM models.
II. The PSD evaluated by the GM/GFM model (with N_2 adsorption/desorption data at 77 K) and trimodal-GM model (with CO_2 adsorption data at 273 K) are comparable to those obtained by DFT and VBS methods.
III. DFT methods take into account the effect of pore geometry on pore filling mechanism and the underlying of pore condensation, and the proposed models only assume monolayer formation followed by multilayer formation. Nevertheless, the reported results in this work are similar to those obtained using DFT methods, highlighting the use of the Grand Canonical formalism in statistical mechanics for the PSD evaluation.

Acknowledgements This research has been partially supported by the research project N MAT2015-68394-R from MINECO (Spain).

References

Barrera, D., Villarroel-Rocha, J., Marenco, L., Oliva, M., Sapag, K.: Non-hydrothermal synthesis of cylindrical mesoporous materials: influence of the surfactant/silica molar ratio. Adsorpt. Sci. Technol. **29**, 975–988 (2011)

Barrett, E.P., Joyner, L.G., Halenda, P.P.: The determination of pore volume and area distributions in porous substances. I. Computations from nitrogen isotherms. J. Am. Chem. Soc. **73**, 373–380 (1951)

Barroso-Bujans, F., Palomino, P., Fernandez-Alonso, F., Rudić, S., Alegría, A., Colmenero, J., Enciso, E.: Intercalation and confinement of poly (ethylene oxide) in porous carbon nanoparticles with controlled morphologies. Macromolecules **47**, 8729–8737 (2014)

Bergaoui, M., Khalfaoui, M., Villarroel-Rocha, J., Barrera, D., Al-Muhtaseb, S., Enciso, E., Sapag, K., Ben Lamine, A.: New insights on estimating pore size distribution of latex particles: statistical mechanics approach and modeling. Microporous Mesoporous Mater. **224**, 360–371 (2016)

Chan, L., Cheung, W., Allen, S., McKay, G.: Error analysis of adsorption isotherm models for acid dyes onto bamboo derived activated carbon. Chin. J. Chem. Eng. **20**, 535–542 (2012)

Chu, W.C., Chiang, S.F., Li, J.G., Kuo, S.W.: Mesoporous silicas templated by symmetrical multiblock copolymers through evaporation-induced self-assembly. RSC Adv. **4**, 784–793 (2014)

Dollimore, D., Heal, G.: Pore-size distribution in typical adsorbent systems. J. Colloid Interface Sci. **33**, 508–519 (1970)

Garrido, J., Linares-Solano, A., Martin-Martinez, J., Molina-Sabio, M., Rodriguez-Reinoso, F., Torregrosa, R., Use of nitrogen vs. carbon dioxide in the characterization of activated carbons. Langmuir **3**, 76–81 (1987)

Gelb, L.D., Gubbins, K.: Pore size distributions in porous glasses: a computer simulation study. Langmuir **15**, 305–308 (1999)

Gregg, S., Sing, K.: Adsorption, Surface Area and Porosity. Academic Press, New York (1982)

Grehov, V., Kalnacs, J., Mishnev, A., Kundzins, K.: Nitrogen adsorption on graphene sponges synthesized by annealing a mixture of nickel and carbon powders. Latv. J. Phys. Tech. Sci. **54**, 36–48 (2017)

Guillet-Nicolas, R., Ahmad, R., Cychosz, K.A., Kleitz, F., Thommes, M.: Insights into the pore structure of KIT-6 and SBA-15 ordered mesoporous silica—recent advances by combining physical adsorption with mercury porosimetry. New J. Chem. **40**, 4351–4360 (2016)

Huang, B., Bartholomew, C.H., Woodfield, B.F.: Improved calculations of pore size distribution for relatively large, irregular slit-shaped mesopore structure. Microporous Mesoporous Mater. **184**, 112–121 (2014)

Jagiello, J., Olivier, J.P.: 2D-NLDFT adsorption models for carbon slit-shaped pores with surface energetical heterogeneity and geometrical corrugation. Carbon **55**, 70–80 (2013)

Jagiello, J., Thommes, M.: Comparison of DFT characterization methods based on N_2, Ar, CO_2, and H_2 adsorption applied to carbons with various pore size distributions. Carbon **42**, 1227–1232 (2004)

Jahandar Lashaki, M., Atkinson, J.D., Hashisho, Z., Phillips, J.H., Anderson, J.E., Nichols, M.: The role of beaded activated carbon's pore size distribution on heel formation during cyclic adsorption/desorption of organic vapors. J. Hazard. Mater. **315**, 42–51 (2016)

Joshi, H.C., Kumar, R., Singh, R.K., Lal, D.: Preparation and characterization of molecular sieving carbon by methane and benzene cracking over activated carbon spheres. Carbon Lett. **8**, 12–16 (2007)

Kakei, K., Ozeki, S., Suzuki, T., Kaneko, K.: Multi-stage micropore filling mechanism of nitrogen on microporous and micrographitic carbons. J. Chem. Soc. Faraday Trans. **86**, 371–376 (1990)

Kaneko, K., Suzuki, T., Kakei, K.: Phase transition of nitrogen molecules filled in micropores of micrographitic carbons. Langmuir **5**, 879–881 (1989)

Kapoor, A., Yang, R.: Correlation of equilibrium adsorption data of condensible vapours on porous adsorbents. Gas Sep. Purif. **3**, 187–192 (1989)

Khalfaoui, M., Knani, S., Hachicha, M., Ben Lamine, A.: New theoretical expressions for the five adsorption type isotherms classified by BET based on statistical physics treatment. J. Colloid Interface Sci. **263**, 350–356 (2003)

Kruk, M., Jaroniec, M., Sayari, A.: Application of large pore MCM-41 molecular sieves to improve pore size analysis using nitrogen adsorption measurements. Langmuir **13**, 6267–6273 (1997)

Landers, J., Gor, G.Y., Neimark, A.V.: Density functional theory methods for characterization of porous materials. Colloids Surf. A **437**, 3–32 (2013)

Leo, W.R.: Statistics and the Treatment of Experimental Data, Techniques for Nuclear and Particle Physics Experiments, pp. 81–113. Springer, New York (1994)

Li, Z., Jin, Z., Firoozabadi, A.: Phase behavior and adsorption of pure substances and mixtures and characterization in nanopore structures by density functional theory. SPE J. **19**, 1096–1109 (2014)

Nagaraju, K., Reddy, R., Reddy, N.: A review on protein functionalized carbon nanotubes. J. Appl. Biomater. Funct. Mater. **13**, e301–e312 (2015)

Nakai, K., Yoshida, M., Sonoda, J., Nakada, Y., Hakuman, M., Naono, H.: High resolution N_2 adsorption isotherms by graphitized carbon black and nongraphitized carbon black—αs-curves, adsorption enthalpies and entropies. J. Colloid Interface Sci. **351**, 507–514 (2010)

Nakhli, A., Khalfaoui, M., Aguir, C., Bergaoui, M., M'henni, M.F., Ben Lamine A.: Statistical physics studies of multilayer adsorption on solid surface: adsorption of basic blue 41 dye onto functionalized Posidonia biomass. Sep. Sci. Technol. **49**, 2525–2533 (2014)

Neimark, A.V., Lin, Y., Ravikovitch, P.I., Thommes, M.: Quenched solid density functional theory and pore size analysis of micro-mesoporous carbons. Carbon **47**, 1617–1628 (2009)

Nicholson, D.: Simulation of adsorption in model microporous graphite, In: Rodriguez-Reinoso, F., Rouquerol, J., Sing, K.S.W., Unger, K.K. (eds.) Studies in Surface Science and Catalysis, pp. 11–20. Elsevier, Amsterdam (1991)

Pekala, R.: Organic aerogels from the polycondensation of resorcinol with formaldehyde. J. Mater. Sci. **24**, 3221–3227 (1989)

Pierce, C.: Computation of pore sizes from physical adsorption data. J. Phys. Chem. **57**, 149–152 (1953)

Prehal, C., Koczwara, C., Jäckel, N., Amenitsch, H., Presser, V., Paris, O.: A carbon nanopore model to quantify structure and kinetics of ion electrosorption with in situ small angle X-ray scattering. Phys. Chem. Chem. Phys. **19**, 15549–15561 (2017)

Przepiórski, J., Czyżewski, A., Pietrzak, R., Toyoda, M., Morawski, A.W.: Porous carbon material containing CaO for acidic gas capture: preparation and properties. J. Hazard. Mater. **263**, 353–360 (2013)

Ravikovitch, P.I., Vishnyakov, A., Russo, R., Neimark, A.V.: Unified approach to pore size characterization of microporous carbonaceous materials from N_2, Ar, and CO_2 adsorption isotherms. Langmuir **16**, 2311–2320 (2000)

Reichhardt, N.V., Guillet-Nicolas, R., Thommes, M., Klösgen, B., Nylander, T., Kleitz, F., Alfredsson, V.: Mapping the location of grafted PNIPAAM in mesoporous SBA-15 silica using gas adsorption analysis. Phys. Chem. Chem. Phys. **14**, 5651–5661 (2012)

Rodriguez-Reinoso, F., Linares-Solano, A.: Chemistry and Physics of Carbon. Marcel Dekker, New York (1988)

Rouquerol, F., Rouquerol, J., Sing, K.: Adsorption by Powders and Porous Solids: Principles, Methodology and Applications. Academic Press, London (1999)

Rouquerol, J., Rouquerol, F., Llewellyn, P., Maurin, G., Sing, K.S.: Adsorption by Powders and Porous Solids: Principles, Methodology and Applications. Academic Press, San Diego (2013)

Seaton, N., Walton, J.: A new analysis method for the determination of the pore size distribution of porous carbons from nitrogen adsorption measurements. Carbon **27**, 853–861 (1989)

Seo, M., Kim, S., Oh, J., Kim, S.-J., Hillmyer, M.A.: Hierarchically porous polymers from hyper-cross-linked block polymer precursors. J. Am. Chem. Soc. **137**, 600–603 (2015)

Sevilla, M., Parra, J.B., Fuertes, A.B.: Assessment of the role of micropore size and N-doping in CO_2 capture by porous carbons. ACS Appl. Mater. Interfaces **5**, 6360–6368 (2013)

Sing, K.S.: Reporting physisorption data for gas/solid systems with special reference to the determination of surface area and porosity (recommendations 1984). Pure Appl. Chem. **57**, 603–619 (1985)

Sun, J.: Pore size distribution model derived from a modified DR equation and simulated pore filling for nitrogen adsorption at 77 K. Carbon **40**, 1051–1062 (2002)

Tan, Z., Gubbins, K.E.: Adsorption in carbon micropores at supercritical temperatures. J. Phys. Chem. **94**, 6061–6069 (1990)

Tao, Y., Endo, M., Kaneko, K.: Hydrophilicity-controlled carbon aerogels with high mesoporosity. J. Am. Chem. Soc. **131**, 904–905 (2009)

Thommes, M., Kaneko, K., Neimark, A.V., Olivier, J.P., Rodriguez-Reinoso, F., Rouquerol, J., Sing, K.S.: Physisorption of gases, with special reference to the evaluation of surface area and pore size distribution (IUPAC Technical Report). Pure Appl. Chem. **87**, 1051–1069 (2015)

Villarroel-Rocha, J., Barrera, D., Sapag, K.: Improvement in the pore size distribution for ordered mesoporous materials with cylindrical and spherical pores using the Kelvin equation. Top. Catal. **54**, 121–134 (2011)

Villarroel-Rocha, J., Barrera, D., Sapag, K.: Introducing a self-consistent test and the corresponding modification in the Barrett, Joyner and Halenda method for pore-size determination. Microporous Mesoporous Mater. **200**, 68–78 (2014)

Wongkoblap, A., Intomya, W., Somrup, W., Charoensuk, S., Junpirom, S., Tangsathitkulchai, C.: Pore size distribution of carbon with different probe molecules. Eng. J. **14**, 45–56 (2010)

Zeller, M., Lorrmann, V., Reichenauer, G., Wiener, M., Pflaum, J.: Relationship between structural properties and electrochemical characteristics of monolithic carbon xerogel-based electrochemical double-layer electrodes in aqueous and organic electrolytes. Adv. Energy Mater. **2**, 598–605 (2012)

Zhang, B., Xing, Y., Li, Z., Zhou, H., Mu, Q., Yan, B.: Functionalized carbon nanotubes specifically bind to α-chymotrypsin's catalytic site and regulate its enzymatic function. Nano Lett. **9**, 2280–2284 (2009)

Zhang, L., Yang, X., Zhang, F., Long, G., Zhang, T., Leng, K., Zhang, Y., Huang, Y., Ma, Y., Zhang, M.: Controlling the effective surface area and pore size distribution of sp^2 carbon materials and their impact on the capacitance performance of these materials. J. Am. Chem. Soc. **135**, 5921–5929 (2013)

Zhang, X., Gao, B., Creamer, A.E., Cao, C., Li, Y.: Adsorption of VOCs onto engineered carbon materials: a review. J. Hazard. Mater. **338**, 102–123 (2017)